Reactions of $\{[Pd(\mu\text{-}SC_6F_5)(\mu\text{-dppm})Pd](\mu\text{-}SC_6F_5)\}_4\cdot 2O(C_2H_5)_2$. Crystal Structures of the Complexes $[(Ph_3P)Pd(\mu\text{-}SC_6F_5)(\mu\text{-dppm})Pd(SC_6F_5)]\cdot 1.4CH_2Cl_2$ and $[(Ph_3P)Pd(\mu\text{-}SC_6F_5)(\mu\text{-dppm})Pd(PPh_3)]SO_3CF_3\cdot 2CH_2Cl_2$ and *ab Initio* MO Calculations on the Model Systems $[(H_3P)Pd(\mu\text{-}H_2PCH_2PH_2)(\mu\text{-SH})Pd(PH_3)]^+$ and $[(H_3P)Pd(\mu\text{-}H_2PCH_2PH_2)Pd(PH_3)]^{2+}$

Rafael Usón,*[,1a] Juan Forniés,[1a] Javier Fernández Sanz,*[,1b] Miguel A. Usón,[1a] Isabel Usón,[1c] and Santiago Herrero[1a]

Departamento de Química Inorgánica, Instituto de Ciencia de Materiales de Aragón, Universidad de Zaragoza-CSIC, E-50009 Zaragoza, Spain, Departamento de Química Física, Facultad de Químicas, Universidad de Sevilla, E-41012 Sevilla, Spain, and Institut für Anorganische Chemie, Universität Göttingen, Tammanstrasse 4, D-3400 Göttingen, Germany

Received July 11, 1996[⊗]

$\{[Pd(\mu\text{-}SC_6F_5)(\mu\text{-dppm})Pd](\mu\text{-}SC_6F_5)\}_4$ reacts 1:4 with neutral ligands L to give $[LPd(\mu\text{-}SC_6F_5)(\mu\text{-dppm})Pd(SC_6F_5)]$ or 1:8 to form $[LPd(\mu\text{-}SC_6F_5)(\mu\text{-dppm})PdL]^+$ (dppm = bis(diphenylphosphino)methane). These binuclear complexes retain the palladium−palladium bond and the two dissimilar bridging ligands, as demonstrated by the X-ray structural determinations carried out on $[(Ph_3P)Pd(\mu\text{-}SC_6F_5)(\mu\text{-dppm})Pd(SC_6F_5)]\cdot 1.4CH_2Cl_2$ and $[(Ph_3P)Pd(\mu\text{-}SC_6F_5)(\mu\text{-dppm})Pd(PPh_3)]SO_3CF_3\cdot 2CH_2Cl_2$. *Ab initio* calculations on the model systems $[(H_3P)Pd(\mu\text{-}H_2PCH_2PH_2)(\mu\text{-SH})Pd(PH_3)]^+$ and $[(H_3P)Pd(\mu\text{-}H_2PCH_2PH_2)Pd(PH_3)]^{2+}$ show that the metal−metal bond arises mainly from interactions between palladium sp orbitals, which also play a predominant role in the binding with the sulfur bridge.

Introduction

The role of bis(diphenylphospine)methane (dppm) as a constraining ligand that holds metal centers at short distances, favoring unusual formal oxidation states, has been long known. Thus, many binuclear complexes containing the palladium−palladium-bonded "$Pd_2(dppm)_2$" moiety have been synthesized;[2] similar compounds with two different bridging ligands are scarce.

We recently described[3] the synthesis of an octanuclear palladium(I) compound (**1**) that contains four equivalent dipal-

$$4[Pd(dppm\text{-}P,P')(SC_6F_5)_2] + 2Pd_2(dba)_3\cdot CHCl_3 \rightarrow \underset{\mathbf{1}}{\{[Pd(\mu\text{-}SC_6F_5)(\mu\text{-dppm})Pd](\mu\text{-}SC_6F_5)\}_4} + 6dba + 2CHCl_3 \quad (1)$$

dba = 1,5-diphenyl-2,4-pentanedien-3-one

ladium(I) units asymmetrically bridged by bis(diphenylphosphino)methane and a pentafluorobenzenethiolate anion. As shown from X-ray diffraction data (see Figure 1), the most outstanding features of these moieties arise from the doubly bridged Pd^I-Pd^I structure. In it, two palladium(I) ions are simultaneously bridged through dppm and a sulfur center, giving rise to an unusual bicyclic structure. The noticeable structure of this compound prompted us to examine both the reactivity and the electronic structure of the bonds involved. The various reaction possibilities (the thiolato bridges, the presumably strained Pd_2S cycles, the metal−metal bonds) of this species make it an interesting subject for reactivity studies, especially if the reaction target can be chosen.

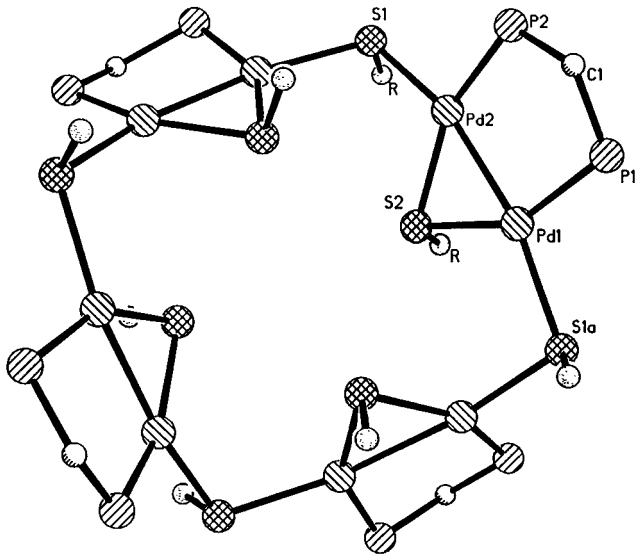

Figure 1. View of compound **1**. Phenyl groups are omitted and only the *ipso* carbons of the thiolates are shown for the sake of clarity.

From a theoretical point of view, electronic properties of metal−metal bonds have been the subject of considerable high-level theoretical work. However, as far as the Pd^I-Pd^I bond is concerned, only a few semiempirical calculations have been reported.[4−7] The large number of Pd^I-Pd^I binuclear complexes known makes it worthwhile to undertake a more reliable, high-

[⊗] Abstract published in *Advance ACS Abstracts,* March 15, 1997.

(1) (a) Instituto de Ciencia de Materiales de Aragón. (b) Universidad de Sevilla. (c) Universität Göttingen.

(2) (a) Chaudret, B.; Delavaux, B.; Poilblanc, R. *Coord. Chem. Rev.* **1988**, *86*, 191−243. (b) Russell, M. J. H.; Barnard, C. F. J. In *Comprehensive Coordination Chemistry*; Wilkinson, G., Gillard, R. D., McCleverty, J. A., Eds.; Pergamon Press Ltd.: Oxford, England, 1987; Vol. 5, pp 1103−1111. (c) Canty, A. J. In *Comprehensive Organometallic Chemistry*; Abel, E. W., Stone, F. G. A., Wilkinson, G., Eds.; Pergamon Press Ltd.: Oxford, England, 1995; Vol. 9, pp 225−227.

(3) Usón, R.; Forniés, J.; Falvello, L. R.; Usón, M. A.; Usón, I.; Herrero, S. *Inorg. Chem.* **1993**, *32*, 1066−1067.

S0020-1669(96)00818-X CCC: $14.00

Table 1. Elemental Analyses and Molar Conductivities of Complexes **2**−**8**

no.	complex	found (calcd) % C	% H	% S	Λ_M[a]
2	$[Pd_2(SC_6F_5)_2dppm(PPh_3)]$	52.73 (52.52)	2.98 (2.97)	5.05 (5.10)	
3	$[Pd_2(SC_6F_5)_2dppm(PCy_3]$	51.82 (51.78)	4.16 (4.34)	5.12 (5.03)	
4	$[Pd_2(SC_6F_5)_2dppm(CO)]\cdot CH_2Cl_2$	42.29 (42.26)	2.05 (2.18)	6.11 (5.79)	
5b	$[Pd_2(SC_6F_5)_2dppm(PPh_3)_2]ClO_4$	56.31 (56.66)	3.71 (3.69)	2.42 (2.26)	128.8
5c	$[Pd_2(SC_6F_5)_2dppm(PPh_3)_2]SO_3CF_3$	55.35 (55.56)	3.49 (3.57)	4.50 (4.36)	126.5
6	$[Pd_2(SC_6F_5)_2dppm(PMePh_2)_2]SO_3CF_3$	51.45 (51.76)	3.70 (3.59)	4.96 (4.77)	112.2
7	$[Pd_2(SC_6F_5)_2dppm(AsPh_3)_2]SO_3CF_3\cdot CH_2Cl_2$	50.65 (50.45)	3.33 (3.31)	4.14 (3.90)	114.6
8	$[Pd_2(SC_6F_5)_2dppm(SbPh_3)_2]SO_3CF_3$	49.09 (49.45)	3.08 (3.17)	4.09 (3.88)	110.9

[a] Ω^{-1} cm^2 mol^{-1}.

level theoretical analysis of this bond, first, and to then study how it is perturbed when a thiolato group bridges the Pd^I-Pd^I unit.

In this paper, we report the reactivity of compound **1** and the theoretical calculations on models based on Pd^I_2 and the Pd^I_2S cycle. The paper is arranged as follows: First, some reactions of compound **1** that preserve the "Pd(μ-SC_6F_5)(μ-dppm)Pd" unit are described. Characterizations of the obtained compounds by both spectroscopic (NMR, IR, MS) and X-ray diffraction techniques are presented. Then a theoretical analysis based on *ab initio* Hartree−Fock calculations on Pd^I_2 and Pd^I_2S models is reported. In this analysis, optimized geometries and vibrational frequencies are provided and compared with experimental results. Finally, the main conclusions are outlined.

Experimental Section

Unless otherwise stated, all reactions were routinely carried out under dry nitrogen, at room temperature, in solvents purified by standard procedures. The compound $\{[Pd(\mu\text{-}SC_6F_5)(\mu\text{-dppm})Pd](\mu\text{-}SC_6F_5)\}_4\cdot 2O(C_2H_5)_2$ was prepared as previously reported.[3]

C, H, and S analyses were performed with a Perkin-Elmer 2400 microanalyzer. IR spectra were recorded (over the range 4000−250 cm^{-1}) on Perkin-Elmer 833 and 1730 FT spectrophotometers, using Nujol mulls between polyethylene sheets.[8] ^{19}F and ^{31}P NMR spectra of $CDCl_3$ solutions of the compounds were run on a Varian XL-200 or UNITY 300 spectrometer, and chemical shifts are relative to $CFCl_3$ and external 85% H_3PO_4, respectively. Conductivities of $\sim 5 \times 10^{-4}$ M acetone solutions were measured with a Philips PW9509 apparatus, using a PW9550/60 cell. Mass spectrometric data were obtained using FAB^+ and FAB^- techniques on a VG Autospec apparatus. The matrix used was 3-nitrobenzyl alcohol, and the samples were dissolved in CH_2Cl_2.

Elemental analyses and molar conductivities are given in Table 1.

Synthesis of [(Ph_3P)Pd(μ-SC_6F_5)(μ-dppm)Pd(SC_6F_5)] (2). To a dichloromethane (25 mL) solution containing 0.0525 g (0.2 mmol) of PPh_3 was added 0.2065 g (0.05 mmol) of $\{[Pd(\mu\text{-}SC_6F_5)(\mu\text{-dppm})Pd](\mu\text{-}SC_6F_5)\}_4\cdot 2O(C_2H_5)_2$. After 3 h of stirring, the solvent was evaporated and the residue was treated with a mixture of diethyl ether (3 mL) and hexane (5 mL). The solid obtained was filtered off, washed with hexane (2 × 3 mL), and dried *in vacuo*. Yield: 89%. IR (cm^{-1}): 1633 w, 1619 w, 1587 w, 1573 w, 1512 vs, 1437 vs, 1309 w, 1274 vw, 1184 m, 1160 w, 1098 vs, 1083 vs, 1027 m, 999 m, 977 vs, 918 w, 855 vs, 781 s, 739 s, 692 vs, 519 vs, 506 s, 489 m, 456 m. ^{19}F NMR: δ −131.8 (d, J_{om} = 25 Hz, F_o), −133.4 (d, J_{om} = 22 Hz, F_o), −164.1 (m, F_m), −158.3 (t, J_{mp} = 21 Hz, F_p), −166.3 (m, $F_m + F_p$). ^{31}P NMR: δ 10.1 (dd, J_{ab} = 63 Hz, J_{ac} = 51 Hz, P_a), 3.9 (dd, J_{bc} = 32 Hz, P_b), 0.0 (dd, P_c). MS(FAB^+), *m/z*: 2317 (2M − SC_6F_5, 4%), 2054 (2M − SC_6F_5 − PPh_3, 2%), 1791 (2M − SC_6F_5 − 2PPh_3, 7%), 1321 (M − SC_6F_5 + PPh_3, 10%), 1059 (M − SC_6F_5, 11%), 860 (M − SC_6F_5 − dppm − Ph + PPh_3, 6%), 797 (M − SC_6F_5 − PPh_3, 12%), 707 (M − C_6F_5 − dppm, 12%), 689 (M − Pd − SC_6F_5 − PPh_3, 12%), 339 (PPh_4, 100%).

Synthesis of [(Cy_3P)Pd(μ-SC_6F_5)(μ-dppm)Pd(SC_6F_5)] (3). To a solution of 0.0713 g (0.2 mmol) of Cy_3PCS_2 in 15 mL of dichloromethane was added 0.2065 g (0.05 mmol) of $\{[Pd(\mu\text{-}SC_6F_5)(\mu\text{-dppm})Pd](\mu\text{-}SC_6F_5)\}_4\cdot 2O(C_2H_5)_2$. After 1 h of stirring, the solution was concentrated to 3 mL, and 40 mL of pentane was added. The precipitated solid was filtered off, washed with 5 mL of pentane, and suction-dried. Prolonged drying *in vacuo* was necessary for the total removal of CS_2. Yield: 74%. IR (cm^{-1}): 1631 w, 1589 w, 1576 w, 1512 s, 1312 vw, 1268 vw, 1192 w, 1175 vw, 1163 w, 1130 m, 1101 m, 1084 s, 1050 s, 1027 w, 1001 s, 978 s, 918 w, 888 w, 851 s, 777 w, 694 s, 676 w, 624 w, 583 w, 523 m, 503 m, 490 w, 340 w. ^{19}F NMR: δ −131.0 (d, J_{om} = 25 Hz, F_o), −133.4 (d, J_{om} = 23 Hz, F_o), −163.7 (m, F_m), −157.3 (t, J_{mp} = 20 Hz), −166.5 (m, $F_m + F_p$). ^{31}P NMR: δ 27.1 (dd, J_{ab} = 61 Hz, J_{ac} = 51 Hz, P_a), 4.8 (dd, J_{bc} = 34 Hz, P_b), −2.8 (dd, P_c). MS(FAB^+), *m/z*: 2354 (2M − SC_6F_5, 37%), 2072 (2M − SC_6F_5 − PCy_3, 21%), 1791 (2M − SC_6F_5 − 2PCy_3, 26%), 1276 (M, 62%), 1077 (M − SC_6F_5, 68%), 689 (M − Pd − SC_6F_5 − PCy_3, 100%). MS(FAB^-), *m/z*: 1195 (M − PCy_3 + SC_6F_5, 30%), 996 (M − PCy_3, 19%), 703 (M − Pd − dppm − PCy_3 + SC_6F_5, 83%), 504 (M − Pd − dppm − PCy_3, 100%).

Synthesis of [(SC_6F_5)Pd(μ-CO)(μ-dppm)Pd(SC_6F_5)] (4). A 0.1033 g sample (0.025 mmol) of $\{[Pd(\mu\text{-}SC_6F_5)(\mu\text{-dppm})Pd](\mu\text{-}SC_6F_5)\}_4\cdot 2O(C_2H_5)_2$ was suspended in 40 mL of dichloromethane, and CO was bubbled through the suspension for 1 h. The resulting dark solution was gravity-filtered and evaporated to 4 mL at 0 °C. After the addition of hexane (40 mL), the solid was filtered off, washed with hexane (2 mL), and dried in a stream of carbon monoxide. Yield: 34%. IR (cm^{-1}): 1897 s, br, 1511 vs, 1439 vs, 1098 s, 1081 s, 972 s, 857 s, 768 m, br, 691 s, 517 m, 503 m, 478 m. ^{19}F NMR: δ −131.6 (d, J_{om} = 27 Hz, F_o), −165.0 (m, F_m), −162.0 (t, J_{mp} = 21 Hz). ^{31}P NMR: δ −6.5 (s).

Synthesis of [(Ph_3P)Pd(μ-SC_6F_5)(μ-dppm)Pd(PPh_3)]ClO_4 (5b). *Caution! Perchlorate salts of metal complexes with organic ligands are potentially explosive. Only small amounts of these materials should be prepared, and they should be handled with great care.*

(a) A 0.1991 g sample (0.048 mmol) of $\{[Pd(\mu\text{-}SC_6F_5)(\mu\text{-dppm})Pd](\mu\text{-}SC_6F_5)\}_4\cdot 2O(C_2H_5)_2$ was added to a dichloromethane (10 mL) solution of 0.0415 g (0.2 mmol) of $Ag(ClO_4)$ and 0.1049 g (0.4 mmol) of PPh_3. After 17 h of stirring, the $Ag(SC_6F_5)$ precipitate was filtered off and the solvent was removed. The crude orange solid was recrystallized from dichloromethane (1 mL)/hexane (10 mL), washed with hexane (15 mL), and dried *in vacuo* over P_2O_5. Yield: 89%.

(b) To a mixture of 0.2623 g (0.1 mmol) of PPh_3 and 0.2073 g (0.1 mmol) of $Ag(ClO_4)$ in dichloromethane (20 mL) was added 0.1258 g (0.1 mmol) of [(Ph_3P)Pd(μ-SC_6F_5)(μ-dppm)Pd(SC_6F_5)]. After 150 min of stirring, the $Ag(SC_6F_5)$ precipitate was filtered off and the reddish filtrate was evaporated to dryness. The solid so obtained was recrystallized from dichloromethane (1 mL)/hexane (10 mL). Yield: 90%. IR (cm^{-1}): 1639 vw, 1587 vw, 1573 vw, 1511 s, 1435 vs, 1310 w, 1185 vw, 1143 vw, 1094 vs, 1027 w, 999 w, 978 m, 853 m, 784 w, 741 s, 693 vs, 623 m, 520 vs, 507 vw. ^{19}F NMR: δ −131.0 (d, J_{om} = 25 Hz, F_o), −162.6 (m, F_m), −156.5 (t, J_{mp} = 21Hz, F_p). ^{31}P NMR: δ 16.7 (m, P_a), 2.3 (m, P_b). MS(FAB^+), *m/z*: 1321 (M, 100%), 1059

(4) Goldberg, S. Z.; Eisenberg, R. *Inorg. Chem.* **1976**, *15*, 535−541.
(5) Harvey, P. D.; Murtaza, Z. *Inorg. Chem.* **1993**, *32*, 4721−4729.
(6) Tanase, T.; Nomura, T.; Fukushima, T.; Yamamoto, Y.; Kobayashi, K. *Inorg. Chem.* **1993**, *32*, 4578−4584.
(7) Harvey, P. D.; Hubig, S. M.; Ziegler, T. *Inorg. Chem.* **1994**, *33*, 3700−3710.
(8) Usón, M. A. *J. Chem. Educ.* **1990**, *66*, 412.

(M − PPh_3, 39%), 860 (M − dppm − Ph, 23%), 797 (M − $2PPh_3$, 17%), 707 (M − dppm − 3Ph + H, 19%), 689 (M − $2PPh_3$ − Pd, 26%).

Synthesis of [(Ph_3P)Pd(μ-SC_6F_5)(μ-dppm)Pd(PPh_3)]SO_3CF_3 (5c). To a solution of 0.0514 g (0.2 mmol) of $Ag(SO_3CF_3)$ and 0.1049 g (0.4 mmol) of PPh_3 in dichloromethane (30 mL) was added 0.2065 g (0.05 mmol) of {[Pd(μ-SC_6F_5)(μ-dppm)Pd](μ-SC_6F_5)}$_4$·$2O(C_2H_5)_2$, and the mixture was stirred for 105 min. The $Ag(SC_6F_5)$ that formed was filtered off and washed with dichloromethane (3 × 3 mL). The collected filtrate and washings were evaporated to dryness under reduced pressure, the crude solid was just dissolved in dichloromethane (*ca.* 2 mL), and the solution was treated with hexane (12 mL). The tomato red solid thus obtained was filtered off, washed with hexane (2 × 2 mL), and dried *in vacuo* over P_2O_5. Yield: 91%. IR (cm^{-1}): 1640 vw, 1587 vw, 1573 vw, 1512 vs, 1436 vs, 1309 vw, 1185 w, 1097 s, 1085 s, 1030 vs, 1269 vs, 1223 w, 1151 s, 999 w, 978 s, 858 m, 788 m, 743 vs, 693 vs, 521 vs, 506 m, 494 m, 481 m, 638 vs, 366 w. ^{19}F NMR: δ −78.4 (s, SO_3CF_3), −131.1 (d, J_{om} = 26 Hz, F_o), −162.5 (m, F_m), −156.3 (t, J_{mp} = 20 Hz, F_p). ^{31}P NMR: δ 16.7 (m, P_a), 2.3 (m, P_b). MS(FAB^+), *m/z*: 1321 (M, 100%), 1059 (M − PPh_3, 53%), 860 (M − dppm − Ph, 26%), 797 (M − $2PPh_3$, 30%), 707 (M − dppm − 3Ph + H, 30%), 689 (M − $2PPh_3$ − Pd, 28%).

Synthesis of [(Ph_2MeP)Pd(μ-SC_6F_5)(μ-dppm)Pd($PMePh_2$)]SO_3CF_3 (6). To a suspension of 0.0514 g (0.2 mmol) of $Ag(SO_3CF_3)$ in 10 mL of dichloromethane were added first 79 μL (0.42 mmol) of $PMePh_2$ and then 0.2065 g (0.05 mmol) of {[Pd_2(μ-SC_6F_5)(μ-dppm)](μ-SC_6F_5)}$_4$·$2O(C_2H_5)_2$ and a further 10 mL of the same solvent. After 16 h of stirring, the $Ag(SC_6F_5)$ precipitate was filtered off and the solvent was removed. The crude residue was dissolved in 2 mL of dichloromethane, and addition of 20 mL of heptane gave an oil, which was stirred for 8 h. The resulting orange solid was filtered off, washed with 5 mL of pentane, and suction-dried. Yield: 93%. IR (cm^{-1}): 1642 vw, 1587 vw, 1576 vw, 1510 s, 1438 vs, 1307 vw, 1280 vs, 1265 vs, 1225w, 1188 vw, 1156 m, 1132 s, 1103 m, 1080w, 1000 vw, 976 s, 854 m, 789 m, 745 m, 692 m, 637 s, 526 w, 509 s, 490 w, 342 w. ^{19}F NMR: δ −78.4 (s, SO_3CF_3), −131.7 (d, J_{om} = 26 Hz, F_o), −162.9 (m, F_m), −156.8 (t, J_{mp} = 21 Hz, F_p). ^{31}P NMR: δ 2.4 (m, P_a), −2.7 (m, P_b). MS(FAB^+), *m/z*: 1196 (M, 100%), 996 (M − PPh_2Me, 87%), 889 (M − Pd − PPh_2Me, 16%), 797 (M − $2PPh_2Me$, 60%), 689 (M − Pd − $2PPh_2Me$, 43%).

Synthesis of [(Ph_3As)Pd(μ-SC_6F_5)(μ-dppm)Pd($AsPh_3$)]SO_3CF_3 (7). To a solution of 0.1225 g (0.4 mmol) of $AsPh_3$ in 30 mL of dichloromethane were added first 0.2065 g (0.05 mmol) of {[Pd(μ-SC_6F_5)(μ-dppm)Pd](μ-SC_6F_5)}$_4$·$2O(C_2H_5)_2$ and then 0.0514 g (0.2 mmol) of $Ag(SO_3CF_3)$, resulting in a dark amber solution. After 5 h of stirring, the precipitated $Ag(SC_6F_5)$ was filtered off, the solvent was partially evaporated (to *ca.* 2 mL), and 5 mL of pentane was added. The solid thus obtained was filtered off, washed with a further 5 mL of pentane, and suction-dried. Yield: 84%. IR (cm^{-1}): 1640 vw, 1582 w, 1513 s, 1436 vs, 1307 vw, 1272 vs, 1223 w, 1186 vw, 1150 s, 1099 m, 1084 m, 1031 s, 999 w, 978 m, 853 m, 788 w, 739 vs, 692 vs, 637 s, 524 m, 505 vw, 479 s, 329 m. ^{19}F NMR: δ −78.4 (s, SO_3CF_3), −131.3 (d, J_{om} = 23 Hz, F_o), −161.9 (m, F_m), −155.5 (t, J_{mp} = 21 Hz, F_p). ^{31}P NMR: δ 1.2 (s). MS(FAB^+), *m/z*: 1410 (M, 26%), 1102 (M − $AsPh_3$, 34%), 904 (M − SC_6F_5 − $AsPh_3$, 20%), 797 (M − $2AsPh_3$, 100%), 689 (M − Pd − $2AsPh_3$, 17%).

Synthesis of [(Ph_3Sb)Pd(μ-SC_6F_5)(μ-dppm)Pd($SbPh_3$)]SO_3CF_3 (8). To a solution of 0.1412 g (0.4 mmol) of $SbPh_3$ in 30 mL of dichloromethane was added 0.2065 g (0.05 mmol) of {[Pd(μ-SC_6F_5)-(μ-dppm)Pd](μ-SC_6F_5)}$_4$·$2O(C_2H_5)_2$. After 15 min of stirring, 0.0514 g (0.2 mmol) of $Ag(SO_3CF_3)$ was added to give a dark red-orange solution. The mixture was stirred for a further 3 h in the absence of light, and the precipitated $Ag(SC_6F_5)$ was filtered off. The solution was evaporated to dryness, the residue was extracted with 2 mL of dichloromethane, and 40 mL of pentane was added. The resulting precipitate was filtered off, washed with 5 mL of pentane, and suction-dried. Yield: 81%. IR (cm^{-1}): 1639 vw, 1578 w, 1511 vs, 1435 vs, 1305 vw, 1263 vs, 1223 w, 1187 vw, 1150 s, 1100 m, 1084 m, 1067 w, 1031 vs, 998 m, 978 m, 851 m, 785 w, 693 vs, 524 m, 505 vw, 637 vs, 454 m, 350 vw, 277 m. ^{19}F NMR: δ −78.4 (s, SO_3CF_3), −131.2 (d, J_{om} = 24 Hz, F_o), −161.2 (m, F_m), −154.6 (t, J_{mp} = 21 Hz, F_p). ^{31}P NMR: δ 0.2 (s). MS(FAB^+), *m/z*: 2498 (2M − $2SbPh_3$ + SC_6F_5, 3%), 1792 (2M − $4SbPh_3$ + SC_6F_5, 17%), 1503 (M, 44%), 1149 (M − $SbPh_3$, 27%), 950 (M − SC_6F_5 − $SbPh_3$, 24%), 873 (M − SC_6F_5 − $SbPh_3$ − Ph, 33%), 797 (M − $2SbPh_3$, 100%), 521 (M − SC_6F_5 − $2SbPh_3$ − Ph, 33%).

Structure Determinations. Single-crystal X-ray structure determinations were carried out using Stoe-Siemens AED2 diffractometers with graphite-monochromated Mo Kα radiation (λ = 0.710 73 Å). The crystal data and data collection and refinement parameters are summarized in Table 2.

(a) [(Ph_3P)Pd(μ-SC_6F_5)(μ-dppm)Pd(SC_6F_5)]·$1.4CH_2Cl_2$. Slow diffusion (at −28 °C) of hexane into a dichloromethane solution of compound **2** gave four huge parallelepipedic red/green (dichroic) crystals. A fragment was mounted on top of a glass fiber in a drop of HMP lithium grease and rapidly cooled. Heavy-atom methods[9] were used to locate the palladium atoms, while subsequent cycles of least-squares refinements and difference Fourier maps were used to locate the remaining non-hydrogen atoms;[10] hydrogen atoms were placed at geometrically calculated positions and refined "riding" on the corresponding carbon atom, with dependent isotropic displacement parameters.

(b) [(Ph_3P)Pd(μ-SC_6F_5)(μ-dppm)Pd(PPh_3)]SO_3CF_3·$2CH_2Cl_2$. Slow diffusion of diethyl ether into a dichloromethane solution of **5c** gave red plates, one of which was mounted on a glass fiber in a drop of rapidly cooled perfluoropolyether.[11] Data vere collected at constant speed, by following the learned profile method.[12] Heavy-atom methods[9] were used to locate the palladium, sulfur, and phosphorus atoms, while subsequent cycles of least-squares refinements and difference Fourier maps were used to locate the remaining non-hydrogen atoms;[10] hydrogen atoms were placed at geometrically calculated positions, and their positional coordinates were constrained to ride on those of the corresponding carbon atoms, with dependent isotropic displacement parameters. An extended version of SHELXL-93[10] was used in the last least-squares refinement to accommodate the 1757 parameters.

Results and Discussion

Although the octanuclear palladium(I) compound {[Pd(μ-SC_6F_5)(μ-dppm)Pd](μ-SC_6F_5)}$_4$·$2O(C_2H_5)_2$ is stable in the solid state and soluble in most common organic solvents, it rapidly decomposes when taken into solution. On the other hand, in diethyl ether or hexane, where the compound is insoluble, reactions do not take place. Thus, only reactions faster than the decay processes yield clean products, which makes it necessary to add the solid substrate to the already dissolved reactants.

Addition (1:4) of {[Pd(μ-SC_6F_5)(μ-dppm)Pd](μ-SC_6F_5)}$_4$·$2O(C_2H_5)_2$ to a dichloromethane solution of a tertiary phosphine L leads (eq 2) to the formation of the corresponding neutral dipalladium(I) complex.

$$\{[Pd(\mu\text{-}SC_6F_5)(\mu\text{-dppm})Pd](\mu\text{-}SC_6F_5)\}_4 + 4L \rightarrow 4[LPd(\mu\text{-}SC_6F_5)(\mu\text{-dppm})Pd(SC_6F_5)] \quad (2)$$

L = PPh_3(**2**), PCy_3(**3**)

As expected, the ^{19}F NMR spectra of these compounds show, in the region assigned to *ortho*-fluorine nuclei of pentafluorobenzenethiolato groups (−125 to −135 ppm),[13] two doublets, the signals at higher fields being somewhat broad. The ^{31}P NMR spectra are characteristic of AMX spin systems, which requires the phosphorus nuclei of the diphosphine to be chemically inequivalent. The positions of the signals exclude chelate behavior of the dppm ligand.[14]

(9) *SHELXTL PLUS*, release 4.0; Siemens Analytical X-Ray Instruments, Inc.: Madison, WI, 1990.
(10) Sheldrick, G. M. SHELXL-93: A Program for Crystal Structure Refinement. Universität Göttingen, Germany, 1993.
(11) Kottke, T.; Stalke, D. *J. Appl. Crystallogr.* **1993**, *26*, 615−619.
(12) Clegg, W. *Acta Crystallogr.* **1981**, *A37*, 22−28.
(13) Usón, R.; Forniés, J.; Usón, M. A.; Apaolaza, J. A. *Inorg. Chim. Acta* **1991**, *187*, 175−180.

Table 2. Crystal Data for Compounds **2**, **5b**, and **5c**

	2·1.4CH_2Cl_2	**5b**	**5c**·2CH_2Cl_2
formula	$C_{56.4}H_{39.8}Cl_{2.8}F_{10}P_3Pd_2S_2$	"$C_{67}H_{52}ClF_5O_4P_4Pd_2S$"	$C_{70}H_{56}Cl_4F_8O_3P_4Pd_2S_2$
fw	1376.57	1420.28	1639.75
crystal system	monoclinic	orthorhombic	orthorhombic
space group	$P2_1/n$ (No. 14)	$Pca2_1$ (No. 29)	$Pca2_1$ (No. 29)
a (Å)	14.054(2)	28.198(6)	27.804(2)
b (Å)	26.528(5)	17.668(4)	17.659(2)
c (Å)	16.532(2)	28.197(6)	27.795(3)
α (deg)	90	90	90
β (deg)	112.034(12)	90	90
γ (deg)	90	90	90
V (Å^3)	5713.3(14)	14048(5)	13647(2)
Z	4	8	8
d_{calcd} (g cm^{-3})	1.600	1.343	1.596
cryst size (mm^3)	0.57 × 0.53 × 0.49	0.57 × 0.57 × 0.34	0.75 × 0.60 × 0.10
μ (mm^{-1})	0.987	0.727	0.908
transm factors: max, min	0.630, 0.502	0.987, 0.901	0.9449, 0.6486
data collecn instrument	Stoe-Siemens AED2		
radiation	Mo Kα (λ = 0.71073 Å) (graphite monochromated)		
temp (K)	200(2)	173(2)	153(2)
scan method	ω/θ	$\omega/2\theta$	ω
θ collecn range (deg)	2.03−22.51	1.54−23.46	3.02−25.10
no. of unique data	7457	10 583	15 768
no. of obsd reflns	7456	10 558	15 768
no. of params refined	721	875	1757
R1[a] [$I > 2\sigma(I)$] (no. of data)	0.0559 (5769)	0.0984 (5685)	0.0555 (12 873)
wR2[b](all data)	0.1591	0.2412	0.1341
weighting parameters: g_1, g_2[c]	0.0763, 28.6693	0.1554, 50.8462	0.0625, 43.3824
quality of fit[d] (on F^2)	1.097	1.044	1.005
largest shift/esd, final cycle	0.000	0.002	20.588[e]
largest peak, hole (e/Å^3)	1.42, −0.72	1.325, −0.675	0.633, −0.694

[a] $R1 = \sum||F_o| - |F_c||/\sum|F_o|$. [b] $wR2 = [\sum w(F_o^2 - F_c^2)^2/\sum w(F_o^2)^2]^{0.5}$. [c] $w = [\sigma^2(F_o^2) + (g_1P)^2 + g_2P]^{-1}$; $P = [\max(F_o^2;0) + 2F_c^2]/3$. [d] Quality of fit = $[\sum w(F_o^2 - F_c^2)^2/(N_{observns} - N_{params})]^{0.5}$. [e] For U_{23}(Cl(3′)) of the disordered solvent; maximum shift/esd for the atoms of the cations 0.000.

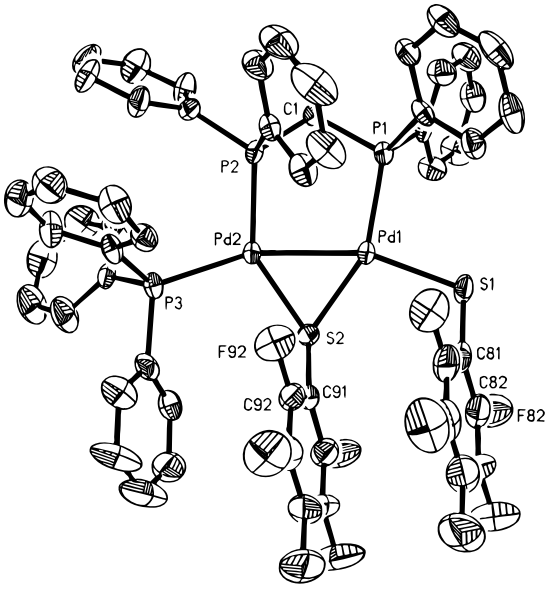

Figure 2. The molecule of compound **2** in the crystal (ellipsoids at 50% electron probability level; other atoms as circles of arbitrary radii; H atoms omitted).

The structure of compound **2** has been established by a single-crystal X-ray diffraction study (see Figure 2 for structure and numbering scheme). Table 3 lists selected atomic positional parameters, and relevant bond distances and angles are given in Table 4. The binuclear complex contains dichloromethane as crystallization solvent, in two different sites (one of them with partial occupation; the other modeled with two alternative positions); bond distance and angle restraints were applied to these molecules.

Table 3. Atomic Coordinates (×10^4) and Equivalent Isotropic Displacement Parameters (Å^2 × 10^3) for **2**[a]

	x	y	z	U(eq)[a]
Pd(1)	797(1)	1940(1)	1899(1)	23(1)
Pd(2)	−515(1)	1770(1)	2640(1)	21(1)
P(1)	1101(2)	2767(1)	2199(1)	24(1)
P(2)	−153(2)	2539(1)	3271(1)	23(1)
P(3)	−1557(2)	1350(1)	3248(1)	28(1)
S(1)	1934(2)	1785(1)	1174(2)	36(1)
S(2)	−228(2)	1235(1)	1645(1)	26(1)
C(1)	123(7)	3019(3)	2577(5)	28(2)

[a] U(eq) is defined as one-third of the trace of the orthogonalized $\mathbf{U}_{ij}$ tensor.

Table 4. Selected Bond Lengths (Å) and Angles (deg) for **2**

Pd(1)−P(1)	2.255(2)	Pd(2)−S(2)	2.321(2)
Pd(1)−S(2)	2.301(2)	Pd(2)−P(3)	2.346(2)
Pd(1)−S(1)	2.366(2)	P(1)−C(1)	1.836(8)
Pd(1)−Pd(2)	2.6068(9)	P(2)−C(1)	1.850(8)
Pd(2)−P(2)	2.260(2)		
P(1)−Pd(1)−S(2)	152.27(8)	S(2)−Pd(2)−P(3)	108.37(8)
P(1)−Pd(1)−S(1)	99.90(8)	P(2)−Pd(2)−Pd(1)	89.18(6)
S(2)−Pd(1)−S(1)	105.20(8)	S(2)−Pd(2)−Pd(1)	55.30(5)
P(1)−Pd(1)−Pd(2)	99.98(6)	P(3)−Pd(2)−Pd(1)	161.53(6)
S(2)−Pd(1)−Pd(2)	56.03(5)	C(1)−P(1)−Pd(1)	108.9(3)
S(1)−Pd(1)−Pd(2)	159.97(7)	C(1)−P(2)−Pd(2)	113.4(3)
P(2)−Pd(2)−S(2)	144.21(8)	Pd(1)−S(2)−Pd(2)	68.67(6)
P(2)−Pd(2)−P(3)	107.41(8)	P(1)−C(1)−P(2)	108.6(4)

If the starting material is considered[3] to be formed by four Pd(μ-SC_6F_5)(μ-dppm)Pd units bridged through four additional pentafluorobenzenethiolato groups to form a 12-membered cycle, compound **2** can be described as the result of cleavage of these bridges by PPh_3; *i.e.*, it contains the same SPd_2P_2C moiety present in the octanuclear precursor **1**.

The five-membered Pd_2P_2C ring is puckered[15] (84% twist with axis through Pd(1) and Pd(2) and 16% envelope with flap

(14) Forniés, J.; Navarro, R.; Urriolabeitia, E. P. *J. Organomet. Chem.* **1990**, *390*, 257−265.

at P(2)) in contrast to the statistically preferred envelope conformation found by Orpen[16,17] for such systems; accordingly, the P(1)−Pd(1)−Pd(2)−P(2) torsion angle (−10.5°) is far from zero. For the six-membered SPd_2P_2C ring, P(2) lies 0.66 Å above and S(2) 0.78 Å under the best plane, described by the carbon, the remaining phosphorus, and both palladium atoms (mean deviation 0.06 Å).

As compared to that of complex **1**, the palladium−palladium bond length (2.607(1) Å) increases slightly, as do the palladium−phosphorus distances to the donor atoms of the bridging diphosphine ligand (Pd(1)−P(1) = 2.255(2) and Pd(2)−P(2) = 2.260(2) Å), which are however shorter than the Pd(2)−P(3) distance of 2.346(2) Å. The terminal ligands do not lie collinear with the palladium−palladium bond (Pd(2)−Pd(1)−S(1) = 160.0 and Pd(1)−Pd(2)−P(3) = 161.5°; torsion angle P(3)−Pd(2)−Pd(1)−S(1) = −8.0°), as has already been found even for symmetrically doubly-bridged $M_2(dppm)_2X_2$ metal−metal-bonded species.[18]

As in the starting octanuclear compound, the perfluorophenyl rings of the thiolato groups are essentially parallel with (dihedral angle 3.45°) and close to each other (mean of the centroid to plane distances 3.34 Å) and the rings are offset (1.05 Å) as a consequence of the polar/π interaction.[19] The aromatic ring of the bridging pentafluorobenzenethiolato group is also roughly parallel with (8.6°) and close to (3.43 Å) a phenyl ring of the triphenylphosphine ligand. The rings are tilted about the $S-C_{ipso}$ bond, forming dihedral angles of 62.6 and 65.9° with the mean SPd_2P_2C plane; the nonbonding distances to the nearest *ortho*-fluorine atoms are however longer (Pd(1)−F(86) = 3.275 and Pd(2)−F(92) = 3.117 Å) than those in the parent compound.

A different type of complex is obtained when the octanuclear complex is treated in dichloromethane with CO (eq 3); although

$$\{[Pd(\mu\text{-}SC_6F_5)(\mu\text{-dppm})Pd](\mu\text{-}SC_6F_5)\}_4 + CO(exc) \rightarrow 4[(SC_6F_5)Pd(\mu\text{-}CO)(\mu\text{-dppm})Pd(SC_6F_5)] \quad (3)$$

4

this is the only species formed, it could not be isolated as a pure solid because it is unstable if not under a carbon monoxide atmosphere.

The ^{19}F NMR spectrum of the reaction solution shows (down to −90 °C) only a doublet in the region assigned to *ortho*-fluorine nuclei of pentafluorobenzenethiolato groups,[13] showing the thiolato groups to be chemically equivalent. The ^{31}P NMR spectrum contains only one peak, which requires the phosphorus nuclei of the diphosphine to be chemically equivalent. The position of the signal excludes chelate behavior of the dppm ligand.[14] Finally, the infrared spectrum of the freshly obtained solid shows a strong broad band at 1897 cm^{-1}, assignable to a CO ligand bridging a Pd^I-Pd^I unit.[20] Starting decomposition can be detected in the infrared spectrum, and a 2-week-old sample shows no bands in the ν(CO) region.

Attempts to grow single-crystals of compound **4**, even using CO-saturated solvents under a carbon monoxide atmosphere, were unsuccessful.

On the other hand, reaction (1:8) between $\{[Pd(\mu\text{-}SC_6F_5)(\mu\text{-dppm})Pd](\mu\text{-}SC_6F_5)\}_4 \cdot 2O(C_2H_5)_2$ and a dichloromethane solution of triphenylphosphine leads to a cationic binuclear complex (eq 4).

$$\{[Pd(\mu\text{-}SC_6F_5)(\mu\text{-dppm})Pd](\mu\text{-}SC_6F_5)\}_4 + 8PPh_3 \rightarrow 4[(Ph_3P)Pd(\mu\text{-}SC_6F_5)(\mu\text{-dppm})Pd(PPh_3)]SC_6F_5 \quad (4)$$

5a

As shown by NMR spectroscopy, the reaction proceeds, in a first fast step, to the formation of the neutral compound **2**, which is converted in a second, slower step to the cationic complex **5a**.

The ^{19}F NMR spectrum of complex **5a** shows in the *ortho*-fluorine region[13] two doublets (1:1); that at higher fields is assignable (*vide infra*) to the free pentafluorobenzenethiolate anion (δ = −132.2 ppm). The ^{31}P NMR spectrum consists of two groups of signals; *i.e.*, in solution and on the NMR time scale both PPh_3 ligands are chemically equivalent, as are both phosphorus nuclei of the diphosphine ligand, which implies an average C_s symmetry of the species or C_2 symmetry along with rapid inversion about the sulfur atom. The spectrum belongs to an AA′XX′ system, but the multiplets are too compressed to allow all the P−P couplings to be ascertained. Chelate coordination of the diphosphine can be discarded from the shift of the signals.[14]

Since this compound could not be isolated as a pure solid, the reaction was repeated in the presence of silver salts of noncoordinating anions in order to exchange the anion (eq 5). The low solubility of $Ag(SC_6F_5)$ not only forces the

$$\{[Pd(\mu\text{-}SC_6F_5)(\mu\text{-dppm})Pd](\mu\text{-}SC_6F_5)\}_4 + 8L + 4AgX \rightarrow 4[LPd(\mu\text{-}SC_6F_5)(\mu\text{-dppm})PdL]X + 4Ag(SC_6F_5) \quad (5)$$

5b,**c**, **6**−**8**

$X = ClO_4$, $L = PPh_3$ (**5b**)

$X = SO_3CF_3$, $L = PPh_3$ (**5c**), $PMePh_2$ (**6**), $AsPh_3$ (**7**), $SbPh_3$ (**8**)

exchange of the counterion but also greatly shortens the completion time (from 5 days to less than 3 h).

The ^{19}F NMR spectra of complexes **5b**,**c** show only one doublet in the *ortho*-fluorine region, corresponding to that at higher frequencies for compound **5a**, whereas the same two multiplets as for compound **5a** are seen in their ^{31}P NMR spectra. The NMR spectra for compounds **6**−**8** are as expected for the above formulation.

Since compound **2** reacts with equimolecular quantities of $Ag(ClO_4)$ and PPh_3 to give compound **5b**, the analogous reaction with 1 mol of PPh_2Me was attempted in order to obtain a mixed-phosphine complex. However, redistribution of the neutral ligands readily occurred and formation of the bis(triphenylphosphine), the bis(diphenylmethylphosphine), and the mixed compound was observed in solution by ^{31}P and ^{19}F NMR spectroscopy and in the mass spectrum of the solid precipitated on addition of hexane. In a similar way, reaction of the octanuclear compound $\{[Pd(\mu\text{-}SC_6F_5)(\mu\text{-dppm})Pd](\mu\text{-}SC_6F_5)\}_4$ with (NBu_4)-Br, in an attempt to synthesize the corresponding anionic dipalladium(I) complex, led to redistribution of the ligands *trans* to the metal−metal bond, and a ternary mixture was observed, which could not be resolved.

A single-crystal X-ray diffraction study of **5b** was attempted. Although the reflections were collected at 200 K and the crystal seemed to be of reasonable quality, a good model could not be

(15) Gould, R. O.; Taylor, P.; Thorpe, M. C. PUCKER. University of Edinburgh, U.K., 1995.
(16) Morton, D. A. V.; Orpen, A. G. *J. Chem. Soc., Dalton Trans.* **1992**, 641−653.
(17) Orpen, A. G. *Chem. Soc. Rev.* **1993**, 191−197.
(18) *Cambridge Structural Database*; Cambridge Crystallographic Data Centre, University Chemical Laboratory: Cambridge, U.K., 1996. See, for instance: Holloway, R. G.; Penfold, B. R.; Colton, R.; McCormick, M. J. *J. Chem. Soc., Chem. Commun.* **1976**, 485−486.
(19) Hunter, C. A.; Sanders, J. K. M. *J. Am. Chem. Soc.* **1990**, *112*, 5525−5534.
(20) Goggin, P. L.; Mink, J. *J. Chem. Soc., Dalton Trans.* **1974**, 534−540.

Table 5. Atomic Coordinates ($\times 10^4$) and Equivalent Isotropic Displacement Parameters ($Å^2 \times 10^3$) for **5c**[a]

	x	*y*	*z*	*U*(eq)[a]
Pd(1A)	9540(1)	8699(1)	10000(1)	23(1)
Pd(2A)	10309(1)	9417(1)	9710(1)	23(1)
P(1A)	8816(1)	8468(1)	10387(1)	26(1)
P(2A)	9630(1)	7778(1)	9446(1)	25(1)
P(3A)	10407(1)	8731(1)	9028(1)	24(1)
P(4A)	10879(1)	10379(1)	9667(1)	29(1)
S(1A)	9876(1)	9713(1)	10389(1)	27(1)
C(31A)	9861(4)	8178(5)	8892(4)	27(2)
Pd(1B)	11605(1)	6438(1)	11389(1)	26(1)
Pd(2B)	10831(1)	5717(1)	11655(1)	29(1)
P(1B)	12327(1)	6677(2)	11005(1)	29(1)
P(2B)	11503(1)	7356(1)	11944(1)	23(1)
P(3B)	10725(1)	6382(2)	12342(1)	29(1)
P(4B)	10258(1)	4753(2)	11685(1)	41(1)
S(1B)	11271(1)	5445(1)	10973(1)	35(1)
C(31B)	11247(4)	6960(6)	12497(4)	29(2)

[a] *U*(eq) is defined as one-third of the trace of the orthogonalized $\mathbf{U}_{ij}$ tensor.

Table 6. Selected Bond Lengths (Å) and Angles (deg) for **5c**

Pd(1A)−P(2A)	2.255(3)	Pd(2A)−S(1A)	2.298(3)
Pd(1A)−S(1A)	2.290(3)	Pd(2A)−P(4A)	2.328(3)
Pd(1A)−P(1A)	2.318(3)	P(2A)−C(31A)	1.811(10)
Pd(1A)−Pd(2A)	2.6136(11)	P(3A)−C(31A)	1.845(11)
Pd(2A)−P(3A)	2.265(3)		
Pd(1B)−P(2B)	2.255(3)	Pd(2B)−S(1B)	2.309(3)
Pd(1B)−S(1B)	2.296(3)	Pd(2B)−P(4B)	2.332(3)
Pd(1B)−P(1B)	2.312(3)	P(2B)−C(31B)	1.834(11)
Pd(1B)−Pd(2B)	2.6090(11)	P(3B)−C(31B)	1.826(11)
Pd(2B)−P(3B)	2.261(3)		
P(2A)−Pd(1A)−S(1A)	147.19(11)	P(3A)−Pd(2A)−S(1A)	150.65(10)
P(2A)−Pd(1A)−P(1A)	106.64(10)	P(3A)−Pd(2A)−P(4A)	105.42(11)
S(1A)−Pd(1A)−P(1A)	105.91(10)	S(1A)−Pd(2A)−P(4A)	103.42(10)
P(2A)−Pd(1A)−Pd(2A)	92.71(8)	Pd(1A)−S(1A)−Pd(2A)	69.45(8)
S(1A)−Pd(1A)−Pd(2A)	55.42(7)	P(2A)−C(31A)−P(3A)	108.9(5)
P(1A)−Pd(1A)−Pd(2A)	159.91(7)		
P(2B)−Pd(1B)−S(1B)	147.40(11)	P(3B)−Pd(2B)−P(4B)	105.07(12)
P(2B)−Pd(1B)−P(1B)	107.09(10)	S(1B)−Pd(2B)−P(4B)	103.93(12)
S(1B)−Pd(1B)−P(1B)	104.91(11)	Pd(1B)−S(1B)−Pd(2B)	69.02(9)
P(3B)−Pd(2B)−S(1B)	150.53(11)	P(3B)−C(31B)−P(2B)	108.9(6)

obtained (best R1 > 9.5%) partly due to pseudosymmetry problems (a noncrystallographic inversion center relates the heavy atoms and most of the carbon atoms of the two independent molecules), but the connectivity was established. Since the crystal system was found to be orthorhombic (as confirmed by oscillation photographs) with $a = c$, twinning (racemic as well as pseudotetragonal) was tried with no better results (the coefficients of the additional components vanished in the least-squares fitting). The perchlorate counterions are disordered over multiple sites, which are assumed to be partially occupied by dichloromethane of solvation as well.

The crystal structure of the homologous compound **5c**, with $CF_3SO_3^-$ as the counterion, was determined at 150 K. Atomic positional parameters for the significant atoms are listed in Table 5, while selected bond distances and angles are given in Table 6. The compound is isostructural with **5b**, crystallizing in the orthorhombic space group $Pca2_1$. The crystal was a racemic twin, with a distribution of 0.5 for each domain. A possible tetragonal twinning was included in the model and discarded, since the population of the additional twinned domains converged to values of 0, within experimental uncertainty.

The asymmetric unit contains four molecules of dichlorometane, three of them disordered. These three were modeled in two alternative sites, with 50% occupancy for each site, but the large displacement parameters along with the high residual electron density in these areas show the situation in the crystal

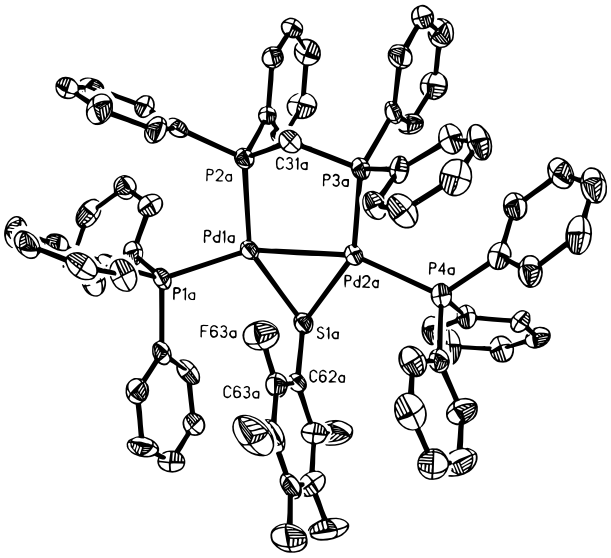

Figure 3. Cation A of compound **5c** in the crystal (ellipsoids at 50% electron probability level; other atoms as circles of arbitrary radii; H atoms omitted).

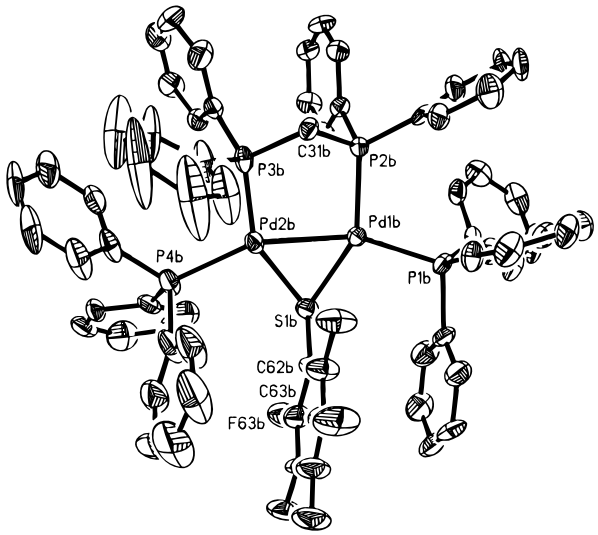

Figure 4. Cation B of compound **5c** in the crystal (ellipsoids at 50% electron probability level; other atoms as circles of arbitrary radii; H atoms omitted).

to be more complex. Attempts to refine more accurate models did not converge. Given the high number of parameters already used in the model, we did not attempt to further account for the C(38B)−C(43B) phenyl ring, which is clearly disordered. Similarity restraints on bond distances, angles, and displacement parameters were applied among both triflate anions and all solvent molecules.

There are two chemically equivalent but symmetry-independent cations per asymmetric unit (see Figures 3 and 4 for structure and numbering scheme), related by a noncrystallographic inversion center, which lies displaced 2.5 Å from the 2_1 axis, where it should be located in the corresponding centrosymmetric group *Pbcm*.

The cations comprise the Pd(μ-SC_6F_5)(μ-dppm)Pd unit present in the octanuclear precursor **1** and the neutral compound **2**, with the two triphenylphosphine ligands *trans* to the metal−metal bond (Figures 3 and 4); the palladium−palladium bond lengths (2.614(1), 2.609(1) Å) are equivalent to the one determined in **2** and slightly longer than that of the starting octanuclear complex **1**. The terminal ligands are not collinear[18] with the palladium−palladium bond, the P−Pd−Pd angles

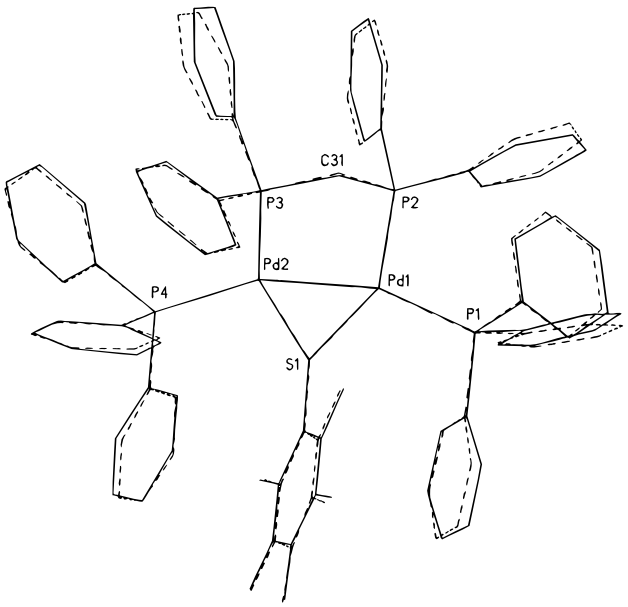

Figure 5. Fit of the two crystallographically independent cations in compound **5c** (mean deviation for $SPd_2P_2P_2C$ = 0.027 Å).

ranging from 158.0 to 159.9°; the P(1)−Pd(1)−Pd(2)−P(4) torsion angles are 9.5 and 4.6°, respectively, for molecules A and B).

The five-membered Pd_2P_2C rings are puckered:[15] 83% twist with the axis through Pd(2A) and P(3A) (66% with the axis through Pd(2B) and P(3B)) and 17% envelope with the flap at P(2A) (34% with the flap at P(2B)); these quite different conformations demonstrate that no authentic inversion center relates both cations in the crystal (as illustrated in Figure 5). These results are again in contrast to the statistically preferred conformation found by Orpen[16,17] in similar systems; accordingly, the P(2)−Pd(1)−Pd(2)−P(3) torsion angles (11.1 for species A and −12.1° for species B) are far from zero. For the SPd_2P_2C core, C(31A) lies 0.48 Å under (0.39 Å for C(31B)) and P(2A) 0.39 Å above (0.44 Å for P(2B)) the best plane, described by the sulfur, the remaining phosphorus, and both palladium atoms (mean deviation 0.02 Å, in both cases).

The aromatic systems in the thiolato ligands are roughly parallel with one phenyl ring of each PPh_3 ligand, describing angles between 6.2 and 13.0°, and the distances between planes are around 3.6 Å. The perfluorophenyl rings are tilted about the $S-C_{ipso}$ bonds, forming dihedral angles of 87.4 (molecule A) and 88.5° (molecule B) with the respective mean SPd_2P_2C planes; the nonbonding distances to the nearest *ortho*-fluorine atoms are Pd(1A)−F(63A) = 3.078 and Pd(1B)−F(67B) = 3.109 Å.

Given the stability of the Pd(μ-SC_6F_5)(μ-dppm)Pd unit, which is maintained in the above described reactions, theoretical calculations were undertaken on this atom assembly. In order to compare the predicted structure with experimentally found results, compound **5c** was chosen; modeling was, however, necessary to diminish the number of variables and make the computations affordable.

Theoretical Calculations

(a) The Models. Because of the high number of atoms and electrons in the [(Ph_3P)Pd(μ-SC_6F_5)(μ-dppm)Pd(PPh_3)] unit, some simplification of the model was necessary. In a first stage, this unit was modeled as a cluster of formula [(H_3P)Pd(μ-$H_2PCH_2PH_2$)(μ-SCF_3)Pd(PH_3)]$^+$, in which the dppm bridge was replaced by diphosphinomethane, the tryphenylphosphine by phosphine, and the pentafluorobenzenethiolato ligand by a trifluoromethanethiolate anion. Preliminary calculations on this structure showed that the computational effort was still too large and that further simplifications would be in order. Single-point calculations, carried out at idealized experimental geometries, showed that replacement of the SCF_3^- bridge by HS^- did not significantly affect the bond properties of the Pd^I_2S cycle; therefore, the [(H_3P)Pd(μ-$H_2PCH_2PH_2$)(μ-SH)Pd(PH_3)]$^+$ cluster was finally adopted as the model. The system without the sulfur bridge was then simply represented by [(H_3P)Pd(μ-H_2PCH_2-PH_2)Pd(PH_3)]$^{2+}$. These models are depicted in Figure 6 and will be designated hereafter as [Pd_2S] and [Pd_2], respectively.

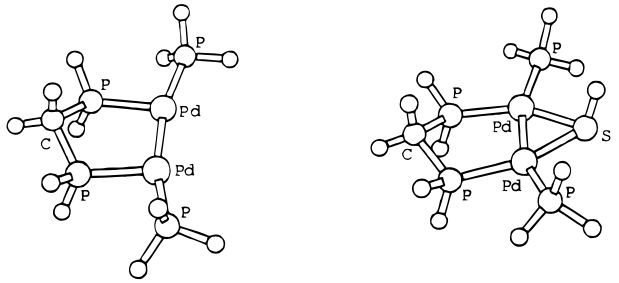

Figure 6. Optimized structures of the [Pd_2] and [Pd_2S] models.

(b) Computational Details. *Ab initio* Hartree−Fock calculations were undertaken, using the effective core potentials (ECP) reported by Stevens *et al.*[21] to describe inner electrons of heavy atoms. For the Pd^I ion, the $4s^2$, $4p^6$, and $4d^9$ electrons were considered, while for P, C, and S, only the valence electrons were explicitly taken into account (70 and 78 electrons for [Pd_2] and [Pd_2S], respectively). The basis set was of sp type with the following contractions: (8s8p5d)/[4s4p3d] for Pd, (4s4p)/[2s2p] for P, C, and S, and (4s)/[2s] for H. For P and S, a set of d polarization functions was added. Molecular geometries were optimized using standard analytical gradient techniques. All the calculations were performed using the HONDO-8 program[22] running on an HP-735 work station.

(c) Molecular Structure. The structural data for compound **5c** (see above) show that the Pd(μ-SC_6F_5)(μ-dppm)Pd moiety is puckered, with a larger twist than envelope component. However, the puckering parameters are quite different for cations A and B (compare Figure 5) showing this to be a packing effect. Besides, the chemical equivalence observed in the ^{31}P NMR spectrum of compound **5c** for the phosphorus nuclei of the triphenylphosphine ligands, as well as for those of the diphosphine, favors a (mean) envelope conformation. Orpen[16,17] has found this to be the most preferred geometry in the solid state for five-membered M_2P_2C rings. According to these data, the geometrical structure of the [Pd_2S] and [Pd_2] models was optimized under C_s constraint; selected geometrical parameters are reported in Table 7, which shows a quite satisfactory agreement with experiment. The interatomic bond distances are systematically found somewhat shorter than the experimental values, although this result seems reasonable considering that the models are much less hindered that the actual complexes. Concerning bond angles, the agreement between the computed values for [Pd_2S] and the mean experimental values is excellent.

When the geometrical parameters of the two models are compared, the most outstanding feature is that the structures of

(21) Stevens, W. J.; Basch, H.; Krauss, M. *J. Chem. Phys.* **1984**, *81*, 6026−6033. Stevens, W. J.; Krauss, M.; Basch, H.; Jasien, P. G. *Can. J. Chem.* **1992**, *70*, 612−630.

(22) Dupuis, M.; Chin, S.; Márquez, A. CHEM-Station and HONDO: Modern Tools for Electronic Structure Studies Including Electron Correlation. In *Relativistic and Electron Correlation Effects in Molecules and Clusters*; Malli, G. L., Ed.; NATO ASI Series; Plenum Press: New York, 1994.

Table 7. Selected Geometrical Parameters for $[Pd_2]$ and $[Pd_2S]$[a]

	Pd−Pd	Pd−P	Pd−P_{exo}	P−C	Pd−S	Pd−Pd−P	Pd−Pd−P_{exo}	C−P−Pd	P−C−P	Pd−S−Pd	τ_C	τ_S
$[Pd_2S]$	2.504	2.157	2.177	1.850	2.222	96.3	161.4	112.7	107.0	68.6	23	174
$[Pd_2]$	2.500	2.158	2.235	1.842		96.5	167.1	111.8	108.5		25	
exp[b]	2.61	2.26	2.32	1.83	2.30	94	159	111	109	69	25	173

[a] Bond distances are in Å, and bond angles in deg. [a] Experimental mean values for units A and B.

Table 8. Mulliken Population Analysis over Shells

	s	p	d	total
		$[Pd_2S]$		
Pd[a]	1.145	1.606	8.134	10.886
P	1.277	2.897	0.314	4.488
P_{exo}	1.298	2.960	0.288	4.547
C	1.084	3.224		4.309
S	1.617	3.853	0.171	5.642
		$[Pd_2]$		
Pd[a]	1.184	1.165	8.127	10.477
P	1.292	2.851	0.316	4.459
P_{exo}	1.313	2.988	0.257	4.557
C	1.098	3.228		4.326

[a] For palladium s and p shells, the values reported are those obtained after subtraction of the $4s^2$ and $4p^6$ electrons.

the five-membered rings are practically the same. This agrees with the well-known stability of the (μ-dppm)Pd^I_2 ring. In fact, significant variations are observed only for bond distances and bond angles involving the *exo* PH_3 ligand.

(d) The Pd^I−Pd^I and Pd^I−S Bonds. The electronic properties of the Pd^I−Pd^I bond have been examined in a small number of theoretical papers, mostly performed using extended Hückel molecular orbital theory (EHMO).[4−7] The main conclusion that arises from these calculations is that the major contribution to the Pd^I−Pd^I σ-bond is from the interaction between palladium d atomic orbitals, with small participation of s and p orbitals (less than 5%). These results suggest that the palladium(I) ion should preserve its d^9 configuration without mixing with $(sp)^1d^8$ type configurations; however, as is well-known, 5s and 5p atomic orbital energies are close to the 4d level and some incorporation of s and p character into the bond would clearly improve the overlap. A second aspect to be considered is that every palladium(I) center is bound to two phosphines (with high σ-donor capabilities[23]) and, therefore, the 5s and 5p Pd^I orbitals have to be partially occupied, while back-donation from Pd^I to phosphorus d orbitals would decrease the d population on the palladium(I) centers.

These expectations are fully confirmed by our *ab initio* Hartree−Fock calculations. As can be observed in Table 8, Mulliken population analysis on the $[Pd_2]$ model gives 8.13 electrons on palladium 4d orbitals and 1.18 and 1.16 on the 5s and 5p orbitals, respectively. Although the use of Mulliken absolute values has been questioned,[24] they clearly agree better with an $(sp)^1d^8$ configuration than with a d^9 configuration.

The analysis of the molecular orbitals (MO's) obtained for $[Pd_2]$ gives a description of the metal−metal bond clearly different from that previously proposed. The MO's involved in the Pd^I−Pd^I bond are the highest nine occupied orbitals. Among these, eight correspond to bonding−antibonding arrangements of d orbitals, while one of them is of bonding sp nature and is easily identified as a σ_{sp} MO. Taking the molecular plane as *xy* and defining the symmetry plane as *xz*,

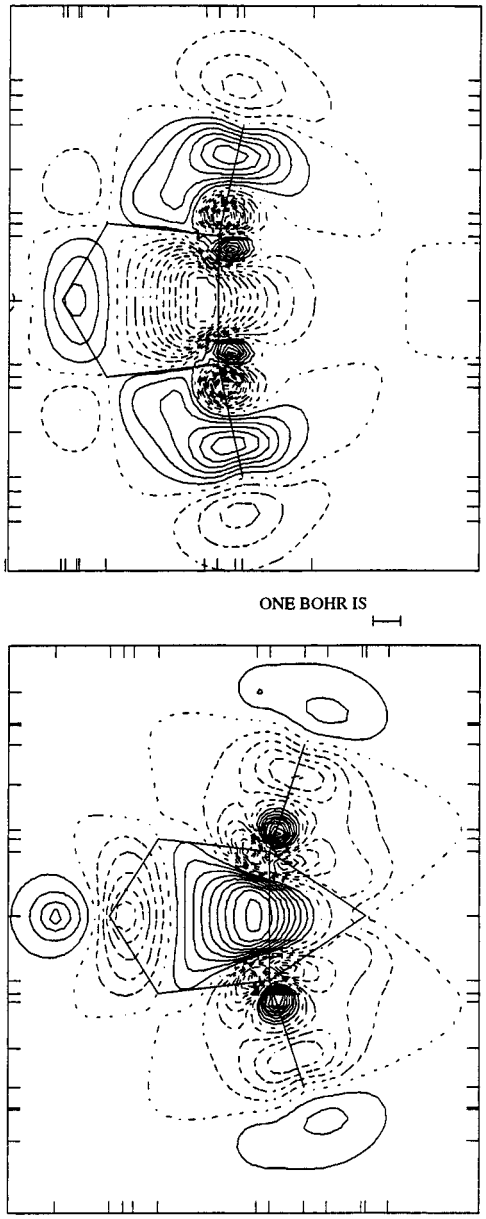

Figure 7. Contour plots for the Pd−Pd σ_{sp} molecular orbitals of $[Pd_2]$ (top) and $[Pd_2S]$ (bottom) structures.

these nine highest MO's are π_{xy}, π_{yz}, δ_{xz}, δ_{xz}*, π_{xy}*, σ_{sp}, π_{zz}, π_{zz}*, and π_{yz}* (ordered by increasing energy). Contour plots for the σ_{sp} MO are reported in Figure 7. As can be seen, this MO lies entirely along the P−Pd−Pd−P line and the main contributions are the p_y orbitals of palladium, while the participation of the Pd $d_{x^2-y^2}$ orbitals is minor, since they are more involved in the bond with phosphines.

It is worthy of note, on the other hand, that EHMO calculations carried out on both $[Pd_2]$ and $[Pd_2S]$ give a description of the palladium−palladium bond in which the $d_{x^2-y^2}$ metal orbitals are preponderant, as had been found by others.[4−6] However, as shown in the present work, higher level calculations lead to a qualitatively different interpretation.

The analysis of the Pd−S bond appears to be quite involved

(23) Puddephatt, R. J.; Dignard-Bailey, L.; Bancroft, G. M. *Inorg. Chim. Acta* **1985**, *96*, L91−L92.

(24) As is well-known, Mulliken population analyses are basis set dependent, and therefore, care should be exercised in their use. See, for instance: Ammeter, J. H.; Bürgi, H. B.; Thibeault, J. C.; Hoffmann, R. *J. Am. Chem. Soc.* **1978**, *100*, 3686−3692. Whangbo, M.-H.; Hoffmann, R. *J. Chem. Phys.* **1978**, *68*, 5498−5500.

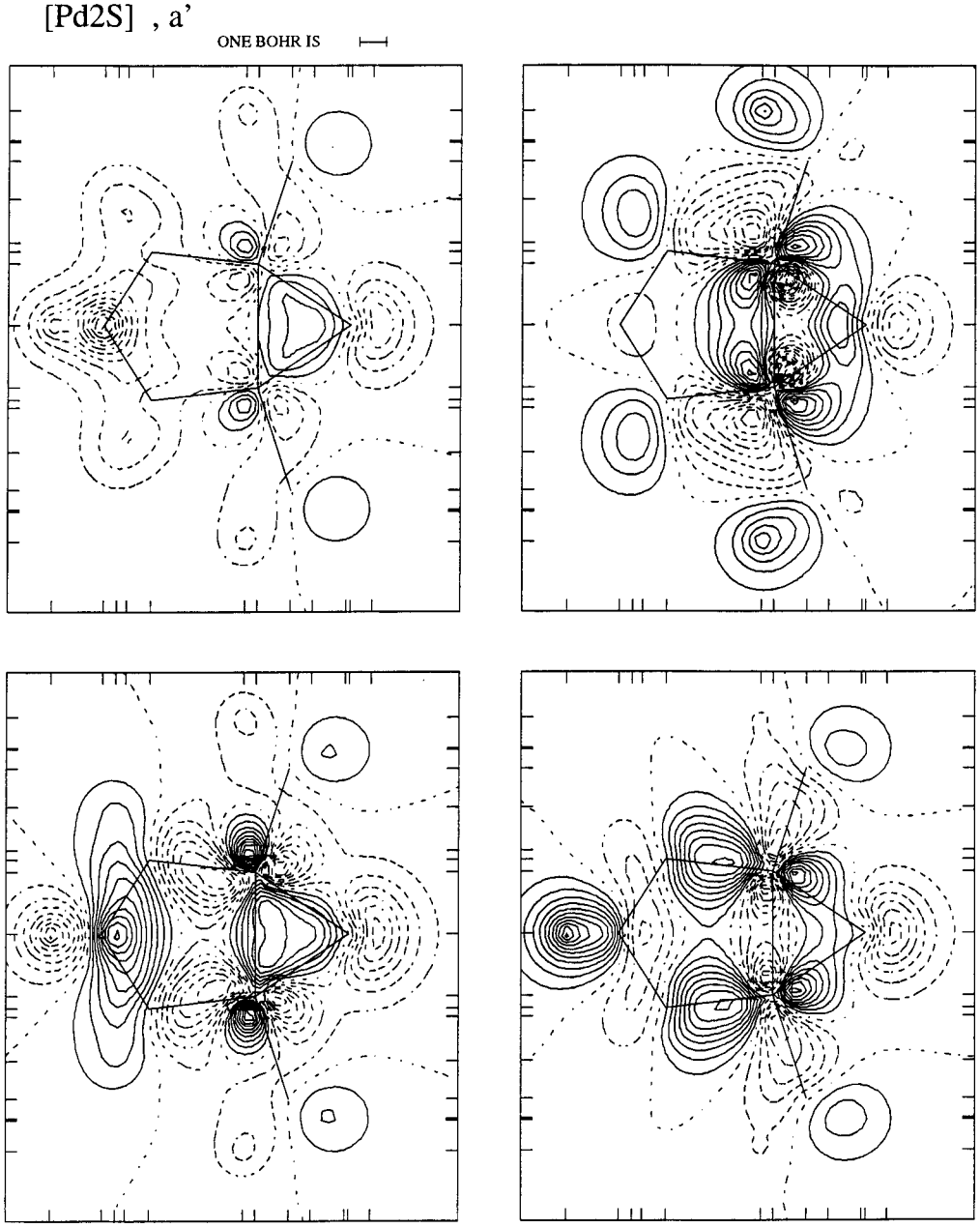

Figure 8. Contour plots for the molecular orbitals arising from the interaction between $[Pd_2]$ and HS^- fragments: (top) $\pi_{xy} \mp sp_x$; (bottom) $d_{x^2-y^2} \mp sp_x$.

since the interaction between the palladium and sulfur orbitals occurs through several MO's and also because the palladium d orbitals are considerably mixed among them. In order to highlight what we think are the main interactions, let us first consider the MO's of an isolated HS^- ligand. The electronic configuration of HS^- is $(C_{\infty v})$ $1\sigma^2 1\sigma^2 1\pi^4$. Under C_s constraint, the σ MO's transform as a′ and the π MO's split into a′ and a″:

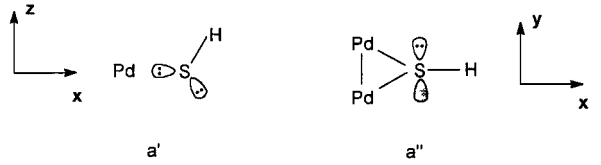

In terms of localized orbitals, the σ_{SH} bond and the sp_z lone pair are not involved in bonding with palladium centers, and only the sp_x (a′) and the p_y (a″) lone pairs have the suitable directionality. Starting with the a′ symmetry orbitals, the main interaction arises from the overlap between the π_{xy} MO of $[Pd_2]$ and the sp_x lone pair of HS^-; when the mix of these orbitals is in phase ($\pi_{xy}-sp_x$ combination), the typical three-center MO is obtained:

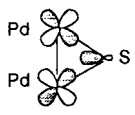

However, for the out-of-phase combination ($\pi_{xy} + sp_x$), there is still some bonding overlap between Pd and S, although in this case such an overlap is of π type and involves the other lobes of palladium d_{xy} orbitals. These interactions can be clearly observed in the contour plots of Figure 8, where bonding overlap is observed in both MO's. A similar feature is found for the interaction of HS^- with the palladium $d_{x^2-y^2}$ orbitals. Depending on the relative sign of the mix, the three-center interaction can be viewed as of σ or π type (see Figure 8).

Combinations of the sulfur p_y orbital with a″ orbitals of $[Pd_2]$, giving rise to a bonding interaction, are depicted in Figure 9.

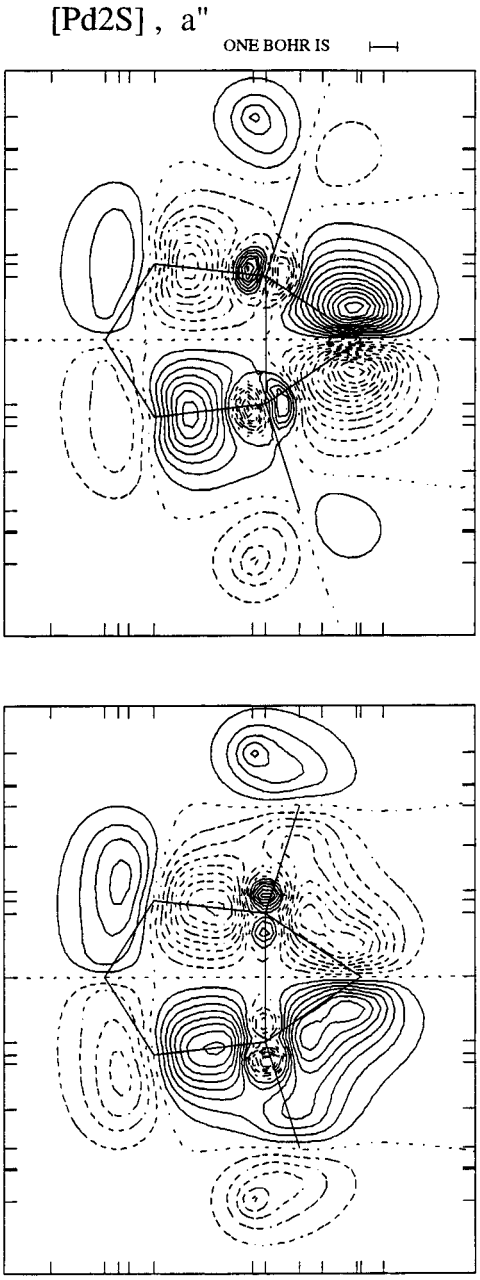

Figure 9. Contour plots for the molecular orbitals arising from the interaction between $[Pd_2]$ and the p_y orbital of HS^-: (top) interaction with palladium sp_x orbitals; (bottom) interaction with $d_{x^2-y^2}$ orbitals.

The main contribution arises from the overlap between the HS^- p_y orbital and an antisymmetric combination of sp_x palladium orbitals (top part of Figure 9). The analysis of this MO may be confusing, since a nodal plane between the palladium and the sulfur centers is observed. However, this node corresponds to the different signs of the inner and outer basis functions representing the $5p_x$ atomic orbital of palladium. The highest coefficient is that of the outer function, which strongly mixes with the sulfur p_y orbital. The second largest interaction of a″ symmetry type arises from the overlap with an antisymmetric combination of the $d_{x^2-y^2}$ metal orbitals (bottom part of Figure 9).

Furthermore, as we have seen in the preceding discussion, the Pd-Pd σ_{sp} MO is not involved in the interaction with the HS^- ligand. This MO is just slightly destabilized upon coordination with sulfur and appears almost "pure" as shown in Figure 7, where the Pd-Pd σ_{sp} MO's of $[Pd_2]$ and $[Pd_2S]$ models are plotted together for the sake of comparison. On the other hand, a careful inspection of the contour plots of the MO's here reported shows that their maxima do not lie on the Pd-S axes. In other words, the charge centroids of these MO's fall out of the ideal three membered ring. This result shows that a nonlinear bond between the palladium and the sulfur centers is established, just like the classical "banana" bonds proposed for the cyclopropane-based rings.

Finally, the charge transfer from the HS^- ligand to the $[Pd_2]$ complex will be addressed. As shown in Table 8, after complexation the total Mulliken populations on Pd centers rise by about 0.4 electron. The largest effect is observed for palladium p orbitals, which increase their population by 0.43 electron each. This trend confirms the preeminent role played by the p metal orbitals in the coordination with the HS^- anion. An additional point concerns the absolute values of the Mulliken populations obtained for the palladium atoms. As can be seen, the total populations are 10.48 and 10.87; *i.e.*, they are two units larger than those expected for a Pd^I cation. Though these values are likely to be overestimated, since in the actual compounds the ligands are phenylphosphines instead of plain PH_3 groups, they reflect the well-known high donor capabilities of phosphines.[23]

(e) Pd−Pd and Pd−S Vibrational Frequencies. Although a full vibrational analysis for both the $[Pd_2]$ and $[Pd_2S]$ models has been carried out, only the frequencies associated with Pd−Pd and Pd−S stretchings will be considered. The vibrational frequencies ω_{Pd-Pd} are computed to be 244 and 253 cm^{-1} for $[Pd_2]$ and $[Pd_2S]$ (harmonic), respectively. These values are in reasonable agreement with an experimental peak observed at 213 cm^{-1} in the Raman spectrum of compound **5c**; they are at higher energy than those found[25] for $Pd_2(dppm)_2X_2$ compounds, whose palladium−palladium bonds are however longer. Although the difference between the theoretical values found for $[Pd_2]$ and $[Pd_2S]$ is almost negligible, the increment found after coordination with sulfur seems to disagree with the fact that the calculated bond order diminishes from 1.14 for $[Pd_2]$ to 0.95 for $[Pd_2S]$ and also with the slight lengthening in the Pd−Pd interatomic bond distance. This apparent discrepancy may be understood by considering that the normal coordinate associated with the Pd−Pd stretching incorporates some Pd_2−S stretching internal coordinate; *i.e.*, the normal coordinate involves displacements of the entire three-membered ring. This mix gives rise to two a′ normal modes: one in which the atoms move in phase (mainly r_{Pd-S}) and the other with displacements out of phase (mainly r_{Pd-Pd}).

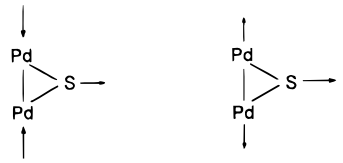

As a consequence, the ω_{Pd-Pd} frequency rises while ω_{Pd-S} decreases. The value computed for the latter is 530 cm^{-1}, in excellent agreement with a peak at 528 cm^{-1} observed in the Raman spectrum.

Conclusions

The reaction of $\{[Pd(\mu\text{-}SC_6F_5)(\mu\text{-dppm})Pd](\mu\text{-}SC_6F_5)\}_4$ with neutral group 15 ligands L affords neutral $[LPd(\mu\text{-}SC_6F_5)(\mu$-

(25) Alves, O. L.; Vitorge, M.-C.; Sourisseau, C. *New J. Chem.* **1983**, *7*, 231−238.

dppm)Pd(SC_6F_5)] or cationic [LPd(μ-SC_6F_5)(μ-dppm)PdL]$^+$ complexes. These binuclear complexes retain the palladium−palladium bond and the two dissimilar bridging ligands, as demonstrated by the X-ray structural determinations of [(Ph_3P)Pd(μ-SC_6F_5)(μ-dppm)Pd(SC_6F_5)]·1.4CH_2Cl_2 and [(Ph_3P)Pd(μ-SC_6F_5)(μ-dppm)Pd(PPh_3)]SO_3CF_3·2CH_2Cl_2. The surprising stability of the mixed bridge permits the incorporation of two different ligands, *trans* to the palladium−palladium bond, which is unprecedented in palladium(I) chemistry.

Contrary to the currently accepted d−d formulation of the palladium−palladium bond, based on EHMO calculations, *ab initio* calculations on the model systems [(H_3P)Pd(μ-$H_2PCH_2PH_2$)(μ-SH)Pd(PH_3)]$^+$ and [(H_3P)Pd(μ-$H_2PCH_2PH_2$)Pd(PH_3)]$^{2+}$ show that this bond arises mainly from the interaction between the 5s and 5p orbitals. Coordination of the [Pd_2] unit with sulfur involves three-center MO's in which the largest participation arises from palladium 5s and 5p orbitals and sulfur lone pairs, giving rise to a typical three-atom "banana" bond.

Acknowledgment. This work was supported by the Dirección General de Investigación Científica y Técnica (Proyectos PB95-1247 and PB94-0597). I.U. is grateful to the EU for an HCM postdoctoral fellowship (ERB CHBG 93 0338), and S.H. thanks the Ministerio de Educación y Ciencia for the award of an FPI scholarship.

Supporting Information Available: Complete listings of crystallographic details, atomic coordinates, bond lengths and bond angles, thermal displacement parameters, and calculated H positional parameters for **2** and **5c** (32 pages). Ordering information is given on any current masthead page.

IC960818E